

Research Plan

Timo A. Lähde¹

¹Department of Physics, University of Washington, Seattle, WA 98195–1560, USA

(Dated: January 14, 2009)

Contents

I. Quantum Monte Carlo simulations	1
A. Graphene and its technological applications	1
1. What is graphene?	1
2. Is graphene in vacuum an insulator?	1
3. Is the semimetal-insulator transition in graphene of second order?	2
4. Are four-fermion interactions in graphene relevant?	2
5. Spontaneous chiral symmetry breaking and the conductivity of suspended graphene	2
6. What are the electronic properties of bilayer graphene?	3
7. Does bilayer graphene support a superfluid state?	4
B. The unitary Fermi gas: from atomic traps to neutron stars	4
1. What is the unitary Fermi gas?	4
2. What is the equation of state of the asymmetric Fermi gas?	4
3. Parallel computing strategies	5
II. QCD and hadronic physics	5
A. Properties of the light scalar mesons	5
B. Partially Quenched Chiral Perturbation Theory	6
C. Electromagnetic effects in $dd \rightarrow \alpha\pi^0$	6
D. Effective-range corrections in bosonic few-body systems	6
E. Spectroscopy of heavy quarkonia	6
References	7

I. QUANTUM MONTE CARLO SIMULATIONS

A. Graphene and its technological applications

In collaboration with Joaquín E. Drut, Nandini Trivedi (The Ohio State University) and Allan H. MacDonald (University of Texas, Austin).

1. What is graphene?

Graphene, a single graphite layer, is a two-dimensional allotrope of carbon that presents several unusual electronic properties [1–4]. In particular, the low-energy spectrum of graphene exhibits a two-fold degeneracy in the band structure, so-called “Dirac cones”, where the

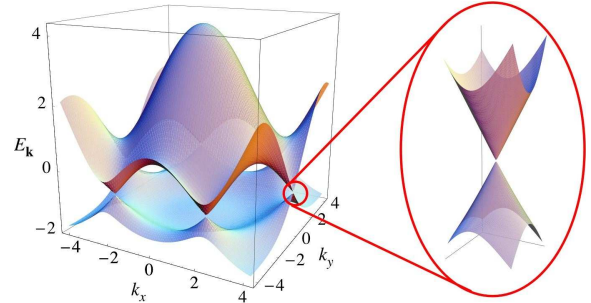


FIG. 1: (from Ref. [3]) Schematic view of the band structure of graphene, zoomed in on a Dirac point, where the valence and conduction bands touch. The low-energy excitations in graphene are thus massless quasiparticles with linear dispersion. Six Dirac points exist in the Brillouin zone due to the hexagonal honeycomb arrangement of the carbon atoms, although only two of the Dirac points are independent.

conduction and valence bands touch. The dispersion around these points is linear, giving rise to quasirelativistic low-energy excitations which move with a velocity $v \ll c$, experimentally determined to be $\sim 10^6$ m/s. As a consequence of the low Fermi velocity, the strength of the Coulomb interaction between these quasiparticles is very large, which precludes a perturbative expansion in the coupling strength. However, the effective Coulomb coupling can be tuned by depositing the graphene sheet on substrates with different dielectric constants.

2. Is graphene in vacuum an insulator?

The low-energy effective theory of graphene possesses a chiral $U(4)$ symmetry which, if the Coulomb interaction between the quasiparticles is sufficiently strong, can spontaneously break, thereby inducing a transition from a semimetallic into an insulating phase [5–11]. Due to the strength of the Coulomb interaction, the problem of determining the critical coupling β_c for this transition is essentially non-perturbative, such that the applicability of analytical methods is limited. We have employed a Lattice Monte Carlo (MC) calculation using Staggered fermions [12–14] in order to establish the existence of a transition, and to study the phase diagram of graphene as a function of the inverse Coulomb coupling β and the number of four-component fermion flavors N_f . These calculations entail the MC simulation of a fermion action in 2+1 dimensions and a gauge (Coulomb) action in 3+1 dimensions, on cubic lattices of dimension up to $L = 18$. Our recent results [15] shown in Fig. 2 indicate

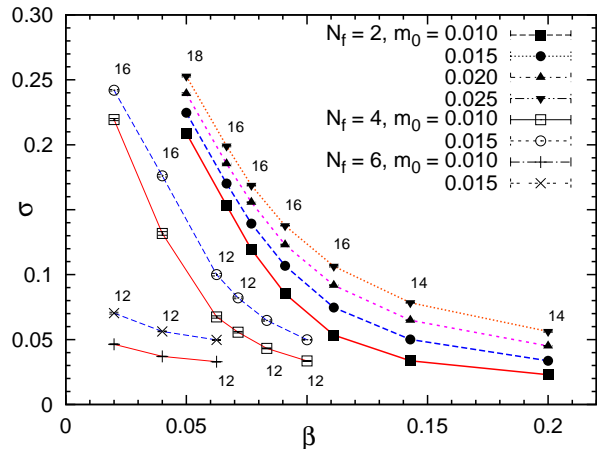


FIG. 2: Chiral condensate σ for $N_f = 2, 4, 6$ as a function of β and m_0 , with lines intended to guide the eye. The lattices are of extent $L^3 \times L_z$, such that the fermions live in a 2+1 dimensional cube of size L , while the gauge bosons also propagate in the z -direction of length L_z . For each β , the value of L is given next to the datapoints. All results are for $L_z = 8$, as larger values had no discernible effects. For each datapoint ~ 300 uncorrelated gauge configurations were generated. The statistical uncertainties, which are comparable to the size of the symbols, were obtained by the jackknife method. Finite volume effects are largest for small β .

that graphene in vacuum (where the Coulomb coupling attains its largest value) should undergo a transition into the insulating phase. In contrast, graphene on a substrate is typically in the semimetallic phase, due to the screening of the Coulomb interaction by the dielectric.

3. Is the semimetal-insulator transition in graphene of second order?

It was found in the non-perturbative study of Ref. [15] that a sufficiently strong Coulomb interaction can induce a quantum transition of the normally semimetallic graphene into an insulating phase. Further, it was argued that the Coulomb interaction in vacuum is likely strong enough to induce such a transition which, within the context of a lattice field theory description, manifests itself as a spontaneous breaking of chiral symmetry, yielding a gap in the quasiparticle spectrum. From an experimental point of view, graphene is thus expected to undergo a semimetal-insulator phase transition when the substrate supporting the graphene sheet (and screening the quasiparticle interaction strength) is removed.

While the phenomenon of spontaneous chiral symmetry breaking in graphene was originally explored by Miransky and collaborators in Ref. [9], the qualitative nature of that study makes it difficult to predict from those results whether actual graphene would undergo such a transition or not, or what the exact properties of the putative transition would be. In particular, the transi-

tion predicted in Ref. [9] is characterized by an essential singularity (also referred to as an infinite-order or Kosterlitz-Thouless transition), as opposed to a power-law singularity typical of second-order phase transitions. In the context of graphene and other similar quantum field theories the occurrence of an essential singularity at a chiral symmetry breaking transition is also referred to as “Miransky scaling”.

As the existence as well as the critical coupling of the semimetal-insulator transition in graphene has been established, the next step is to determine whether the transition is of second order or of Kosterlitz-Thouless type, as suggested by solution of the gap equation [7–9]. However, our recent results [15] for the chiral susceptibility appear to be consistent with a second-order transition. In order to obtain a conclusive result, simulations closer to the chiral limit, as well as for larger lattice volumes are required. Studies in these directions, as well as applications for computer time at NERSC [17], TeraGrid [18] and the Ohio Supercomputer Center (OSC) [19] are currently in progress. A Hybrid Monte Carlo (HMC) algorithm is also being implemented, which will allow for simulations on much larger lattices, as well as for better scaling on parallel machines.

4. Are four-fermion interactions in graphene relevant?

The simulational studies of Ref. [15] have focused on the effects of the Coulomb interaction in graphene, which is expected to be the dominant contributor to the structure of the phase diagram. However, it is conceivable that zero-range four-fermion interactions may alter this picture in a non-trivial way, since the possibility exists that such contributions may become relevant at strong coupling. So far, such effects have only been studied in the $1/N_f$ expansion [20–22], but have not yet been non-perturbatively investigated, which is also true of the velocity renormalization in graphene due to the Coulomb interaction. The (perturbative) $1/N_f$ expansion suggests that four-fermion interactions should remain small at strong coupling, but on the other hand this is true also for the Coulomb interaction, such that the observed semimetal-insulator transition appears to be a truly non-perturbative effect. Ultimately, the question of whether four-fermion interactions alter the quantitative structure of the phase diagram of graphene can only be settled by a rigorous non-perturbative analysis, such as a simulation using the Lattice Monte Carlo technique.

5. Spontaneous chiral symmetry breaking and the conductivity of suspended graphene

The conductivity of graphene is directly related to the issue of spontaneous chiral symmetry breaking in graphene, as it can yield information on whether the system is in a semimetallic or insulating phase at low tem-

peratures. For some time, conductivity measurements in graphene samples deposited on a substrate indicated (see Refs. [1–3]) an approximately temperature-independent value of the minimal (DC) conductivity $\sigma^{\min} \simeq 4e^2/h$, which turned out to be difficult to reconcile with the values around e^2/h found by several approximate analytic studies (see Refs. [23–33]; Ref. [34] provides an overview of theoretical estimates).

However, recent progress [35, 36], in the experimental study of suspended graphene samples (see Fig. 3) in combination with current-annealing techniques to dramatically increase the carrier mobility and reduce the concentration of impurities, has revealed that intrinsic graphene actually shows a remarkable non-metallic behavior at low temperatures, as indicated by a sharp rise in the resistivity as the temperature is lowered (see Fig. 4). Such behavior not only invalidates the earlier descriptions providing evidence for a temperature-independent conductivity, but moreover also disagrees sharply with more recent studies [37]. While the non-metallic behavior of the conductivity at low T may be interpreted as the first evidence for an insulating phase in graphene as predicted in Ref. [15, 16], it may conceivably also be due to finite-size effects [38]. Nevertheless, as pointed out in Ref. [39], a complete study of the electrical response of graphene should account for non-perturbative effects, and is therefore well suited for a Monte Carlo approach. The calculation of the minimal DC conductivity of graphene has not yet been attempted with such a technique, which is also of relevance for the study of high- T_c superconductors [40].

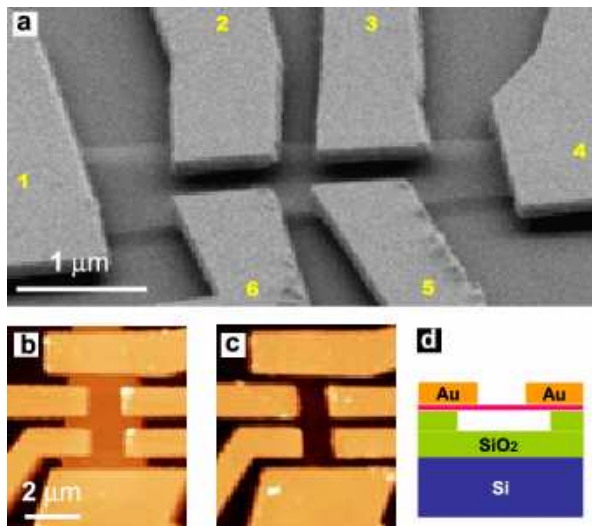


FIG. 3: Illustration of suspended graphene (from Ref. [35]). The manufacturing process consists of several steps: Firstly, sheets of graphene are deposited on an SiO_2 substrate, whereafter the underlying substrate is etched away, leaving the graphene sheet suspended over a trench. Finally, Au electrodes are deposited lithographically. A detailed description of this process can be found in Ref. [36].

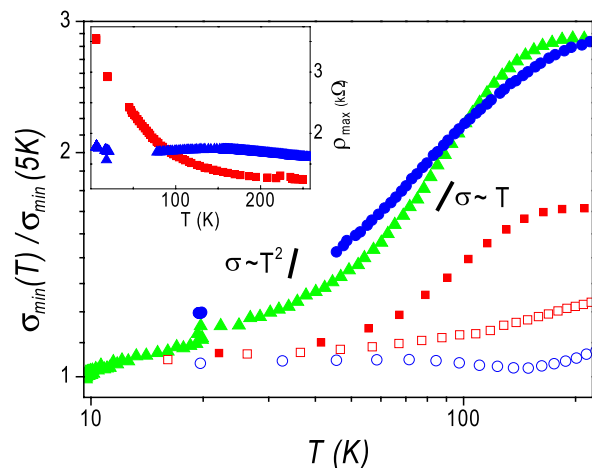


FIG. 4: Measurement of the conductivity and resistivity in suspended graphene (from Ref. [35]). In the inset, the triangles and squares indicate the resistivity before and after annealing, respectively. This experiment reveals that the roughly constant and temperature-independent resistivity is not an intrinsic property of graphene. In contrast, the annealed sample shows a markedly non-metallic behavior, suggestive of an insulating phase at low T .

The determination of the DC conductivity of graphene requires the evaluation of a four-point correlation function at large Euclidean time, and an analytic continuation to Minkowski time. The evaluation of four-point correlation functions is a routinely performed task in the computation of the chiral condensate susceptibility of graphene. Only relatively minor modifications to existing routines are necessary in order to obtain the correlation function relevant for the DC conductivity. On the other hand, analytic continuation to Minkowski time is a non-trivial procedure that applies not only to the conductivity, but also to other related response functions. Fortunately, in the case of the conductivity, a method has been developed by Ref. [41] which allows for the extraction of the low-frequency (DC) limit without necessitating a full-fledged analytic continuation. This method, which is being implemented for the study of graphene, has in the past been successfully applied to a superconductor-insulator transition in a disordered electronic system.

6. What are the electronic properties of bilayer graphene?

In the context of potential electronic applications of graphene, perhaps the most important player is the bilayer form, because of the possibility of opening a gap in the spectrum already at relatively weak Coulomb coupling. Indeed, it is in fact a requirement for many applications is that it be possible to open such a gap. In the band theory of bilayer graphene, a gap is opened up by placing the bilayer in a perpendicular electric field which makes a potential difference between the two layers. This

kind of electric field is routinely made in electronics by means of gates. From the theoretical perspective, however, the study of bilayer graphene poses a similar set of problems as presented by monolayer graphene, in that the strength of the Coulomb interaction precludes a non-perturbative treatment. As a consequence, details such as the precise value of the gap, are unknown from first principles at this time. If simulations at finite chemical potential turn out to be feasible, the phenomenon of Coulomb drag in bi-layer graphene [42] may also be addressed.

7. Does bilayer graphene support a superfluid state?

It has recently been proposed [43] that the application of an external potential difference between two graphene layers may result in an infrared instability, described by BCS theory which leads to a broken symmetry with spontaneous phase coherence. Such exciton condensation has hitherto only been seen in the context of the quantum Hall effect [44], although the possibility exists that such a state may form in bilayer graphene at quite high temperatures. This state has superfluid properties which can be revealed experimentally by means of transport experiments where the two layers are contacted separately. However, a reliable estimate of the critical temperature for this effect requires a quantitative Lattice Monte Carlo analysis.

B. The unitary Fermi gas: from atomic traps to neutron stars

In collaboration with Joaquín E. Drut (The Ohio State University).

1. What is the unitary Fermi gas?

Strongly interacting, dilute Fermi gases have lately been at the focus of considerable theoretical and experimental interest [45] in particular due to the technique of using so-called Feshbach resonances [46] to tune the strength of the interaction between fermionic atoms in a trap [47]. This unprecedented situation has allowed for the exploration of the connection between Bose-Einstein condensation (BEC) of composite bosons and Bardeen-Cooper-Schrieffer (BCS) superfluidity of fermionic atoms, thereby improving the understanding of the BEC-BCS crossover [48–51], illustrated in Fig. 5.

Another reason why dilute Fermi gases have been under intense investigation is the existence of the so-called unitary regime, where the average distance between particles is much larger than the range of the interaction, but still much smaller than the scattering length. As a result, the thermodynamic properties are governed by simple laws [53]. In particular, right at the unitary point,

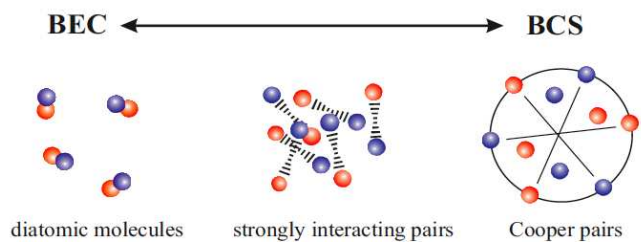


FIG. 5: (from Ref. [52]) Schematic representation of the BEC-BCS crossover. Red and blue (dark and light) atoms represent different spins (\uparrow or \downarrow). In the BEC regime the interaction is strong enough to form well-localized molecules, which undergo Bose-Einstein condensation below a critical temperature. In the deep BCS regime, the weak attraction between the atoms leads, below the critical temperature, to the formation and condensation of Cooper pairs. The intermediate region, where the scattering length is larger than every other scale, is usually referred to as the unitary regime.

where the scattering length is infinite, a dilute gas of fermions is characterized solely by its density [54–56]. However, the absence of scales (other than the density) renders a quantitative treatment very difficult, due to the lack of an obvious small dimensionless parameter in which to construct a perturbative expansion. In spite of this, various analytic treatments have been explored with some degree of success [57–59]. Essentially, the problem of the unitary Fermi gas requires a fully non-perturbative treatment, typically a Monte Carlo simulation, where the uncertainties are ideally of purely statistical origin.

Previous Quantum Monte Carlo (QMC) studies at finite temperature [60–63], some of them performed by the Nuclear Theory group at the UW, have focused on various thermodynamical quantities for the unpolarized unitary Fermi gas, such as the determination of the critical temperature T_c for superfluidity. However, much less is known about the case of unequal densities of spin-up and spin-down particles (the polarized or asymmetric unitary Fermi gas) at finite temperature, although at zero temperature, several possible phase diagrams have been put forward [64–67]. The asymmetric case is also relevant for astrophysical problems such as the structure of neutron stars, where varying densities of neutrons and protons are encountered at different depths inside the star.

2. What is the equation of state of the asymmetric Fermi gas?

Monte Carlo simulations at finite spin-polarization suffer from the notorious “sign problem” which has a detrimental effect on convergence. The severity of the sign problem may vary greatly as a function of the asymmetry $\delta\mu$ and temperature T . Our preliminary studies suggest that extant algorithms for the unpolarized case may be applicable, by means of the standard re-weighting technique [68, 69] out to significant values of $\delta\mu$, depending

on the precise value of T . Our first objective is to perform a QMC simulation to obtain the energy and the chemical potential of the asymmetric Fermi gas for non-zero T and $\delta\mu$, and to study the dependence of the critical temperature T_c for superfluidity as a function of $\delta\mu$, as shown in Fig. 6. Once these objectives have been attained, straightforward extensions include studies of the case of unequal masses as well as of couplings away from unitarity. Also, knowledge of the chemical potential as a function of T enables the use of the Local Density Approximation (LDA), and potentially also more sophisticated flavors of density functional theory, for the calculation of density profiles. These are central for the comparison with experiments using trapped atomic gases, where the system is not spatially homogeneous.

3. Parallel computing strategies

A significant programming effort has already been invested into optimizing and parallelizing existing QMC codes, previously developed by the Nuclear Theory Group at the UW. As a result of these efforts, major progress has been achieved towards larger lattice sizes and improved scalability. The latter point is particularly important since it enables the efficient use of supercomputing facilities. At the time of writing, an application for 3×10^5 processor-hours at the OSC [19] supported

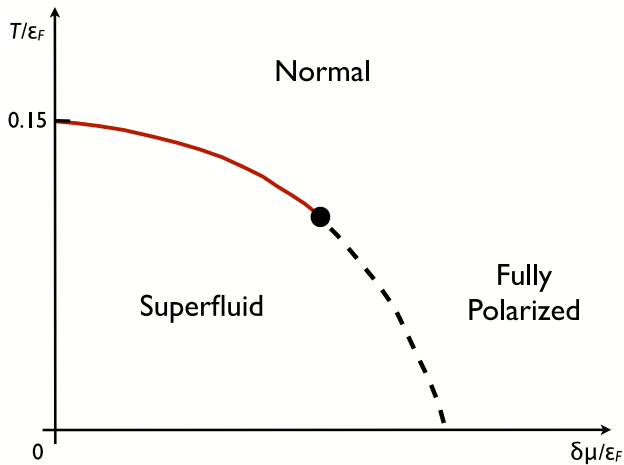


FIG. 6: Schematic phase diagram of the strongly-interacting polarized Fermi gas as a function of the temperature T and the asymmetry $\delta\mu$. For low T the system is in a superfluid phase, and the continuous (red) line represents a second-order phase transition separating the superfluid and normal phases. Simulations have been performed by the NT group at the UW [61, 62], giving $T_c \sim 0.15$ for the case of $\delta\mu = 0$. It is conceivable that for large enough $\delta\mu$, a tricritical point is reached where the line of second-order transitions becomes a line of first-order transitions, as indicated by the dashed (black) line. One of our main objectives is to quantitatively explore this phase diagram away from $\delta\mu = 0$.

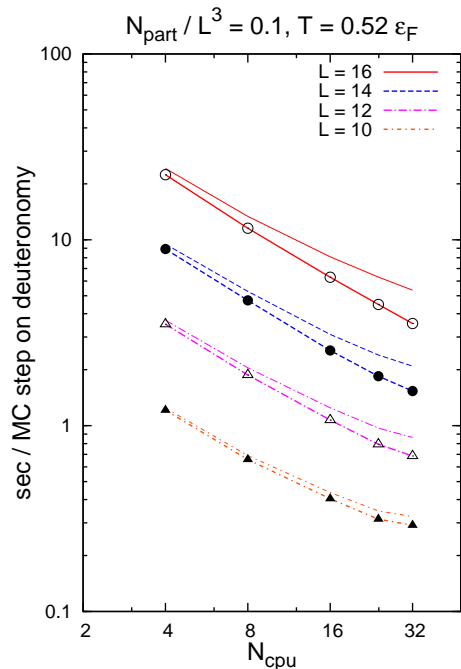


FIG. 7: Timing of the QMC code for large lattices and high temperatures, in which case the sequential parts are most significant. The time taken by the evolution phase of a single MC step for $L = 12$ (full triangles), 14 (open triangles), 16 (full circles) and 18 (open circles) are given as a function of the number of processor cores in a log-log plot. The thin lines (without symbols) show the corresponding data when the time taken by the action calculation is included. The deviations from linear behavior are due to a combination of communication overhead and increasing significance of the sequential parts. These tests were performed on the Intel Xeon cluster “deuteronomy” at the University of Washington.

by R. J. Furnstahl (Ohio State University) has been accepted. As good scaling has been observed (see Fig. 7) on the Intel Xeon clusters “deuteronomy” and “athena” at the UW, an application for further computer time at the TeraGrid [18] is planned. Such good scalability was achieved by minimization of the CPU time used for inherently sequential operations. Further investigations into the use of a Hybrid Monte Carlo (HMC) approach are in progress. If successful, further dramatic improvements in the overall performance of the code can be expected.

II. QCD AND HADRONIC PHYSICS

A. Properties of the light scalar mesons

In collaboration with Bastian Kubis (Bonn University) and José Peláez (Universidad Complutense, Madrid). At low energies, the interactions between S -wave pairs of pions and kaons can be described using the non-perturbative method of unitarization [70–73]. In particular, the so-called Inverse Amplitude Method (IAM) [74]

makes use of the next-to-leading-order (NLO) chiral scattering amplitudes and gives a favorable description of S -wave $\pi\pi$ and $K\bar{K}$ scattering at energies up to and above the $K\bar{K}$ threshold at ~ 1 GeV. The closely related scalar form factors of the pions and kaons have also been obtained using the leading-order (LO) chiral scattering amplitudes and LO [75] or NLO [76] chiral scalar form factors as a starting point. It has recently been shown by Lähde and Meißner [77] that such unitarized scalar form factors may provide an excellent description of recent high-precision experimental data [78] on J/ψ decays into a light vector meson (ω or ϕ) by the emission of a $\pi\pi$ or $K\bar{K}$ pair. In particular, the pattern of isoscalar σ and $f_0(980)$ resonances in the ϕ and ω channels was faithfully reproduced. Our present objective is to provide a unified description of the S -wave $\pi\pi$ and $K\bar{K}$ scattering data and the scalar form factors within the IAM framework. This can potentially yield not only much improved estimates for the masses and widths of the light isoscalar mesons, but also tighter constraints on the low-energy constants (LECs) of QCD. Accurate knowledge of the pion and kaon scalar form factors is also of importance for the analysis of B -meson decays involving the light isoscalar mesons [79].

B. Partially Quenched Chiral Perturbation Theory

In collaboration with Johan Bijnens (Lund University). The low-energy effective theory of QCD, Chiral Perturbation Theory (ChPT) [80–82], depends on a number of *a priori* unknown low-energy constants (LECs). While many quantities, such as the pion mass and decay constant, can nowadays be computed with high precision via Lattice QCD simulations [83], more complicated processes such as semileptonic kaon decays [84, 85] are easier to analyze within the context of ChPT. One possible approach is then to use quantities calculable on the lattice to fix the LECs required for the ChPT analysis of more complicated processes. While present Lattice QCD calculations typically use unphysical light sea-quark masses [86], referred to as partial quenching. This situation can be described within the context of Partially Quenched ChPT (PQChPT), and can actually be beneficial as the extra degree of freedom provided by variation of the sea-quark mass can be used to access more LECs than would otherwise be possible [87, 88]. At present, we have calculated the pseudoscalar meson masses and decay constants [89, 90] to two loops (NNLO) in PQChPT, and provided numerical implementations of the analytically complicated expressions. Possible future directions include the analysis of extant Lattice QCD data using the NNLO PQChPT expressions, the calculation of the finite-volume corrections [91–93] to NNLO, and the calculation of pion and kaon form factors [94–96]. A potential stumbling block is the necessity to extrapolate the lattice QCD data to the continuum limit, although a possible solution is to use formulations such as Staggered

ChPT [97] to directly account for the effects of a finite lattice spacing.

C. Electromagnetic effects in $dd \rightarrow \alpha\pi^0$

In collaboration with Gerald Miller (University of Washington). The effects of initial-state Coulomb interactions in the charge-symmetry-breaking [98, 99] reaction $dd \rightarrow \alpha\pi^0$ [100] were investigated by us [101] in terms of a simplified set of deuteron and α wave functions, and a plane-wave approximation for the initial dd state. In this process, the Coulomb interaction between the two initial-state protons leads to the breakup of the dd pair into a continuum state that is well connected to the final $\alpha\pi^0$ state by the strong emission of a pion. The resulting contribution to the cross-section was found to be comparable in size to those of previously established mechanisms [102]. Inclusion of the initial-state Coulomb mechanism is therefore desirable in a full calculation, using realistic NN interactions and dd wave functions [102–104].

D. Effective-range corrections in bosonic few-body systems

In collaboration with Hans-Werner Hammer (Bonn University) and Lucas Platter (Ohio State University). Few-body systems with large scattering length a have universal properties that do not depend on the details of their interactions at short distances [105–107]. The rate constant for three-body recombination of bosonic atoms of mass m into a shallow dimer scales as $\hbar a^4/m$ times a log-periodic function of the scattering length [108]. The leading and sub-leading corrections to the rate constant due to the effective range of the atoms were calculated by us [109] via numerical solution of the Skornyakov - Ter-Martirosian (STM) integral equation. As an example, the results were applied to potential model calculations [110] for ${}^4\text{He}$ atoms. The present work has been extended by Platter and Shepard [111] to account for the effects of deep dimers, which allowed for a successful description of recent experimental results [112] for the recombination rate of ultra-cold ${}^{133}\text{Cs}$ atoms.

E. Spectroscopy of heavy quarkonia

In collaboration with Dan-Olof Riska (University of Helsinki), K. O. E. Henriksson and C. J. Nyfält. We have calculated [113–116] the rate of the electromagnetic spin-flip transition $J/\psi \rightarrow \eta_c\gamma$, as well as those of the other electric (E1) and magnetic (M1) dipole transitions in heavy quarkonia, notably charmonium ($c\bar{c}$) and bottomonium ($b\bar{b}$) within a constituent quark model based on the

relativistic Blankenbecler-Sugar reduction [117] of the Bethe-Salpeter equation. Good qualitative agreement with the experimentally determined transition rates [118] was obtained under the assumption that the effective confining interaction is dominated by a Lorentz scalar com-

ponent. However, the usefulness of such an approach is limited by the phenomenological character of the quarkonium potential models and the strongly coupled, relativistic nature of the quarkonia, in particular the heavy-light mesons.

-
- [1] K. S. Novoselov, *Science* **306**, 666 (2004).
 [2] K. S. Novoselov *et al.*, *Proc. Natl. Acad. Sci. U.S.A.* **102**, 10451 (2005); *Nature* (London) **438**, 197 (2005).
 [3] A. K. Geim, K. S. Novoselov, *Nat. Mat.* **6**, 183 (2007).
 [4] A. H. Castro Neto *et al.*, [[arXiv:0709.1163](https://arxiv.org/abs/0709.1163)].
 [5] J. González, F. Guinea, M. A. H. Vozmediano, *Nucl. Phys. B* **424**, 595 (1994); *Phys. Rev. Lett.* **77**, 3589 (1996); *Phys. Rev. B* **59**, 2474(R) (1999).
 [6] O. Vafek, M. J. Case, *Phys. Rev. B* **77**, 033410 (2008).
 [7] D. V. Khveshchenko, *Phys. Rev. Lett.* **87**, 246802 (2001).
 [8] H. Leal, D. V. Khveshchenko, *Nucl. Phys. B* **687**, 323 (2004).
 [9] E. V. Gorbar *et al.*, *Phys. Rev. B* **66**, 045108 (2002).
 [10] A. L. Tchougreeff, R. Hoffmann, *J. Phys. Chem.* **96**, 8993 (1992).
 [11] F. R. Wagner, M.-B. Lepetit, *ibid.* **100**, 11050 (1996).
 [12] J. Kogut, L. Susskind, *Phys. Rev. D* **11**, 395 (1975); *ibid.* **16**, 3031 (1977).
 [13] H. Kluberg-Stern, *Nucl. Phys. B* **220**, 447 (1983).
 [14] C. Burden, A. N. Burkitt, *Eur. Phys. Lett.* **3**, 545 (1987).
 [15] J. E. Drut, T. A. Lähde, *Phys. Rev. Lett.* **102**, 026802 (2009).
 [16] J. E. Drut, T. A. Lähde, [[arXiv:0901.0584](https://arxiv.org/abs/0901.0584)].
 [17] <http://www.nersc.gov>
 [18] <http://www.teragrid.org>
 [19] <http://www.osc.edu>
 [20] I. F. Herbut, *Phys. Rev. Lett.* **97**, 146401 (2006).
 [21] D. T. Son, *Phys. Rev. B* **75**, 235423 (2007).
 [22] J. E. Drut, D. T. Son, *Phys. Rev. B* **77**, 075115 (2008).
 [23] A. W. W. Ludwig, M. P. A. Fisher, R. Shankar, G. Grinstein, *Phys. Rev. B* **50**, 7526 (1994).
 [24] K. Ziegler, *Phys. Rev. B* **55**, 10661 (1997), *Phys. Rev. Lett.* **80**, 3113 (1998).
 [25] M. I. Katsnelson, *Eur. Phys. J. B* **51**, 157 (2006).
 [26] E. V. Gorbar *et al.*, *Phys. Rev. Lett.* **95**, 146801 (2005); *Phys. Rev. B* **73**, 245411 (2006).
 [27] N. M. R. Peres, F. Guinea, A. H. Castro Neto, *Phys. Rev. B* **73**, 125411 (2006).
 [28] J. Tworzydło *et al.*, *Phys. Rev. Lett.* **96**, 246802 (2006).
 [29] J. Cserti, *Phys. Rev. B* **75**, 033405 (2007).
 [30] P. M. Ostrovsky, I. V. Gornyi, A. D. Mirlin, *Phys. Rev. B* **74**, 235443 (2006).
 [31] S. Ryu, C. Mudry, A. Furusaki, A. W. W. Ludwig, [[arXiv:cond-mat/0610598](https://arxiv.org/abs/cond-mat/0610598)].
 [32] L. A. Falkovsky, A. A. Varlamov, [[arXiv:cond-mat/0606800](https://arxiv.org/abs/cond-mat/0606800)].
 [33] K. Ziegler, *Phys. Rev. Lett.* **97**, 266802 (2006).
 [34] K. Ziegler, *Phys. Rev. B* **75**, 233407 (2007).
 [35] K. I. Bolotin *et al.*, *Phys. Rev. Lett.* **101**, 096802 (2008); V. Crespi, *Physics* **1**, 15 (2008).
 [36] K. I. Bolotin *et al.*, *Solid State Commun.* **146**, 351 (2008).
 [37] L. Fritz, J. Schmalian, M. Müller, S. Sachdev, *Phys. Rev. B* **78**, 085416 (2008).
 [38] M. Müller, M. Bräuninger, B. Trauzettel, [[arXiv:0812.4141](https://arxiv.org/abs/0812.4141)].
 [39] D. Liu, S. Zhang, [[arXiv:0803.3488](https://arxiv.org/abs/0803.3488)].
 [40] E. Dagotto, *Rev. Mod. Phys.* **66**, 763 (1994).
 [41] N. Trivedi, R. T. Scalettar, M. Randeria, *Phys. Rev. B* **54**, 3756(R) (1996).
 [42] W.-K. Tse, B. Y.-K. Hu, S. Das Sarma, *Phys. Rev. B* **76**, 081401(R) (2007).
 [43] R. Bistritzer, H. Min, J. J. Su, A. H. MacDonald, [[arXiv:0810.0331](https://arxiv.org/abs/0810.0331)].
 [44] J. P. Eisenstein, A. H. MacDonald, [[arXiv:cond-mat/0404113](https://arxiv.org/abs/cond-mat/0404113)].
 [45] S. Giorgini *et al.*, [[arXiv:0706.3360](https://arxiv.org/abs/0706.3360)]; I. Block, J. Dalibard, W. Zwerger, [[arXiv:0704.3011](https://arxiv.org/abs/0704.3011)].
 [46] U. Fano, *Phys. Rev.* **124**, 1866 (1961); H. Feshbach, *Ann. Phys. (N.Y.)* **19**, 287 (1962);
 [47] K. M. O'Hara *et al.*, *Science* **298**, 2179 (2002); J. Kinast *et al.*, *Science* **307**, 1296 (2005); M. Bartenstein *et al.*, *Phys. Rev. Lett.* **92**, 120401 (2004); M. Bourdel *et al.*, *Phys. Rev. Lett.* **93**, 050401 (2004); G. B. Partridge *et al.*, *Science* **311**, 503 (2006); J. T. Stewart *et al.*, *Phys. Rev. Lett.* **97**, 050401 (2004).
 [48] D. R. Eagles, *Phys. Rev.* **186**, 456 (1969).
 [49] A. J. Leggett, in *Modern Trends in the Theory of Condensed Matter*, edited by A. Pekalski, J. Przystawa, (Springer-Verlag, Berlin, 1980).
 [50] P. Nozières, S. Schmitt-Rink, *J. Low Temp. Phys.* **59**, 195 (1985).
 [51] P. F. Bedaque, H. Caldas, G. Rupak, *Phys. Rev. Lett.* **91**, 247002 (2003).
 [52] C. Regal, D. Jin, [[arXiv:cond-mat/0601054](https://arxiv.org/abs/cond-mat/0601054)].
 [53] T.-L. Ho, *Phys. Rev. Lett.* **92**, 090402 (2004).
 [54] J. Carlson *et al.*, *Phys. Rev. Lett.* **91**, 050401 (2003).
 [55] G. E. Astrakharchik *et al.*, *Phys. Rev. Lett.* **93**, 200404 (2004).
 [56] J. Carlson, S. Reddy, *Phys. Rev. Lett.* **95**, 060401 (2005).
 [57] Y. Nishida, D. T. Son, *Phys. Rev. Lett.* **97**, 050403 (2006).
 [58] P. Arnold, J. E. Drut, D. T. Son, *Phys. Rev. A* **75**, 043605 (2007).
 [59] P. Nikolic, S. Sachdev, *Phys. Rev. A* **75**, 033608 (2007).
 [60] E. Burovski *et al.*, *Phys. Rev. Lett.* **96**, 160402 (2006).
 [61] A. Bulgac, J. E. Drut, P. Magierski, *Phys. Rev. Lett.* **96**, 090404 (2006); *ibid.* **99**, 120401 (2007).
 [62] A. Bulgac, J. E. Drut, P. Magierski, *Int. J. Mod. Phys. B* **20**, 5165 (2006); *Phys. Rev. A* **78**, xxxxx (2008) [[arXiv:0803.3238](https://arxiv.org/abs/0803.3238)].
 [63] A. Bulgac, J. E. Drut, P. Magierski, G. Wlazłowski, [[arXiv:0801.1504](https://arxiv.org/abs/0801.1504)].
 [64] C.-H. Pao, S.-T. Wu, S.-K. Yip, *Phys. Rev. B* **73**,

- 132506 (2006).
- [65] D. T. Son, M. A. Stephanov, Phys. Rev. A **74**, 013614 (2006).
- [66] A. Bulgac, M. M. Forbes, A. Schwenk, Phys. Rev. Lett. **97**, 020402 (2006).
- [67] A. Bulgac, M. M. Forbes, Phys. Rev. A **75**, 031605(R) (2007).
- [68] I. Montvay, G. Münster, *Quantum Fields on the Lattice* (Cambridge University Press, 1994).
- [69] T. DeGrand, C. DeTar, *Lattice Methods for Quantum Chromodynamics* (World Scientific, 2006).
- [70] T. N. Truong, Phys. Rev. Lett. **61**, 2526 (1988); *ibid.* **67**, 2260 (1991);
- [71] A. Dobado, M. J. Herrero, T. N. Truong, Phys. Lett. B **235**, 134 (1990);
- [72] J. A. Oller, E. Oset, J. R. Peláez, Phys. Rev. Lett. **80**, 3452 (1998);
- [73] J. A. Oller, E. Oset, Nucl. Phys. A **620**, 438 (1997), erratum *ibid.* A **652**, 407 (1999).
- [74] A. Gómez Nicola, J. R. Peláez, Phys. Rev. D **65**, 054009 (2002).
- [75] L. Roca, J. E. Palomar, E. Oset, H. C. Chiang, Nucl. Phys. A **744**, 127 (2004)
- [76] Ulf-G. Meißner, J. A. Oller, Nucl. Phys. A **679**, 671 (2001).
- [77] T. A. Lähde, Ulf-G. Meißner, Phys. Rev. D **74**, 034021 (2006).
- [78] M. Ablikim *et al.* [BES collaboration], Phys. Lett. B **607**, 243 (2005); *ibid.* **598**, 149 (2004); *ibid.* **603**, 138 (2004).
- [79] R. Dutta, S. Gardner, [arXiv:0805.1963].
- [80] S. Scherer, *Introduction to chiral perturbation theory*, Advances in nuclear physics **27**, 277, edited by J. W. Negele, E. Vogt, (Kluwer Academic / Plenum Publishers, New York, 2003), [hep-ph/0210398].
- [81] G. Ecker, *Strong interactions of light flavours*, [hep-ph/0011026].
- [82] A. Pich, *Effective field theory*, [hep-ph/9806303].
- [83] S. R. Beane, P. F. Bedaque, K. Orginos, M. J. Savage, Phys. Rev. D **75**, 094501 (2007).
- [84] G. Amorós, J. Bijnens, P. Talavera, Phys. Lett. B **480**, 71 (2000); Nucl. Phys. B **585**, 293 (2000), erratum *ibid.* B **598**, 665 (2001).
- [85] J. Bijnens, P. Talavera, Nucl. Phys. B **669**, 341 (2003).
- [86] S. R. Sharpe, *Applications of chiral perturbation theory to lattice QCD*, [arXiv:hep-lat/0607016].
- [87] C. W. Bernard, M. F. L. Golterman, Phys. Rev. D **49**, 486 (1994).
- [88] S. R. Sharpe, N. Shoresh, Phys. Rev. D **62**, 094503 (2000); *ibid.* **64**, 114510 (2001).
- [89] J. Bijnens, T. A. Lähde, Phys. Rev. D **71**, 094502 (2005); *ibid.* **72**, 074502 (2005).
- [90] J. Bijnens, N. Danielsson, T. A. Lähde, Phys. Rev. D **70**, 111503(R) (2004); *ibid.* **73**, 074509 (2006).
- [91] G. Colangelo, S. Dürr, Eur. Phys. J. C **33**, 543 (2004).
- [92] G. Colangelo, C. Haefeli, Nucl. Phys. B **744**, 14 (2006).
- [93] J. Bijnens, K. Ghorbani, Phys. Lett. B **636**, 51 (2006).
- [94] J. Bijnens, G. Colangelo, P. Talavera, JHEP **9805**, 014 (1998).
- [95] J. Bijnens, P. Talavera, JHEP **0203**, 046 (2002).
- [96] J. Bijnens, P. Dhonte, P. Talavera, JHEP **0401**, 050 (2004); *ibid.* **0405**, 036 (2004).
- [97] C. Aubin, C. Bernard, Phys. Rev. D **68**, 034014 (2003).
- [98] G. A. Miller, B. M. K. Nefkens, I. Šlaus, Phys. Rept. **194**, 1 (1990).
- [99] G. A. Miller, A. K. Opper, E. J. Stephenson, Ann. Rev. Nucl. Part. Sci. **56**, 253 (2006).
- [100] E. J. Stephenson *et al.*, Phys. Rev. Lett. **91**, 142302 (2003).
- [101] T. A. Lähde, G. Miller, Phys. Rev. C **75**, 055204 (2007), erratum *ibid.* **77**, 019904 (2008).
- [102] A. Gärdestig *et al.*, Phys. Rev. C **69**, 044606 (2004).
- [103] A. Nogga *et al.*, Phys. Lett. B **639**, 465 (2006).
- [104] A. Deltuva, A. C. Fonseca, P. U. Sauer, Phys. Rev. C **73**, 057001 (2006).
- [105] V. Efimov, Phys. Lett. B **33**, 563 (1970); Sov. J. Nucl. Phys. **12**, 589 (1971); *ibid.* **29**, 546 (1979).
- [106] P. F. Bedaque, H.-W. Hammer, U. van Kolck, Phys. Rev. Lett. **82**, 463 (1999); Nucl. Phys. A **646**, 444 (1999).
- [107] E. Braaten, H.-W. Hammer, Phys. Rept. **428**, 259 (2006); Ann. Phys. **322**, 120 (2007).
- [108] P. F. Bedaque, E. Braaten, H.-W. Hammer, Phys. Rev. Lett. **85**, 908 (2000).
- [109] H.-W. Hammer, T. A. Lähde, L. Platter, Phys. Rev. A **75**, 032715 (2007).
- [110] K. T. Tang, J. P. Toennies, C. L. Yiu, Phys. Rev. Lett. **74**, 1546 (1995).
- [111] L. Platter, J. R. Shepard, [arXiv:0711.1908].
- [112] T. Kraemer *et al.*, Nature (London) **440**, 315 (2006).
- [113] T. A. Lähde, C. J. Nyfält, D.-O. Riska, Nucl. Phys. A **645**, 587 (1999); *ibid.* **674**, 141 (2000).
- [114] K. O. E. Henriksson *et al.*, Nucl. Phys. A **686**, 355 (2001).
- [115] T. A. Lähde, D.-O. Riska, Nucl. Phys. A **693**, 755 (2001); *ibid.* **707**, 425 (2002); *ibid.* **710**, 99 (2002).
- [116] T. A. Lähde, Nucl. Phys. A **714**, 183 (2003).
- [117] R. Blankenbecler, R. Sugar, Phys. Rev. **142**, (1966) 1051.
- [118] T. Skwarnicki, [arXiv:hep-ex/0505050].